# Modeling terrestrial $^{13}C$ cycling: Climate, land use and fire

M. Scholze,[1,2] P. Ciais,[3] and M. Heimann[4]

Received 20 November 2006; revised 19 July 2007; accepted 19 October 2007; published 7 February 2008.

[1] The LPJ terrestrial carbon isotope model, which includes isotopic fractionation of $^{13}C$ during assimilation and a full description of the isotopic terrestrial carbon cycle, has been used to calculate the atmosphere-biosphere exchange flux of $CO_2$ and its $\delta^{13}C$ for the years 1901 to 1998. A transient, spatially explicit data set of $C_4$ crops and tropical $C_4$ pastures has been compiled. In combination with a land use scheme this allows the analysis of the impact of land use conversion of $C_3$ ecosystems to $C_4$ cultivation, besides climate, fire disturbances, atmospheric $CO_2$ and the isotope ratio of atmospheric $CO_2$, on the terrestrial carbon stable isotope composition. Globally averaged values of modeled leaf discrimination vary between 17.9‰ and 17.0‰ depending on the chosen land use scheme and also the year of the simulation. Results from the simulation experiment prescribing the conversion of $C_3$ ecosystems into $C_4$ crops and $C_4$ pastures show the lowest leaf discrimination. Modeled values of isotopic disequilibrium flux, caused by the $\delta^{13}C$ difference between fixed $CO_2$ and released $CO_2$, similarly depend on the amount of prescribed $C_4$ vegetation and vary between 37.9 Pg C‰ $yr^{-1}$ and 23.9 Pg C‰ $yr^{-1}$ averaged over the years 1985 to 1995. In addition, the effect of fire on the isotopic disequilibrium has been diagnosed; generally wildfires lead to a disequilibrium reduction of ≈10 Pg C‰ $yr^{-1}$ because they shorten the turnover time of terrestrial carbon. If used in a global double deconvolution study, the differences in the results between the standard experiment without any $C_4$ cultivation and the experiment including $C_4$ crops and pastures could account for a shift of about 1 Pg C $yr^{-1}$ from the inferred terrestrial sources to the ocean fluxes.

**Citation:** Scholze, M., P. Ciais, and M. Heimann (2008), Modeling terrestrial $^{13}C$ cycling: Climate, land use and fire, *Global Biogeochem. Cycles*, *22*, GB1009, doi:10.1029/2006GB002899.

## 1. Introduction

[2] Atmospheric $CO_2$ concentrations are driven by anthropogenic emissions (combustion of fossil fuel, biomass burning, and cement manufacture). However, only about half of these emissions stay on average in the atmosphere and cause the increase in atmospheric $CO_2$. The remainder is taken up by the oceans and terrestrial biosphere. An understanding of the mechanisms and also the temporal and spatial patterns of this uptake is of high political and scientific importance in the context of future carbon emissions [*Prentice et al.*, 2001].

[3] Measurements of atmospheric $CO_2$ and its isotopic composition expressed as $\delta^{13}C$ which is calculated as the deviation with respect to a standard: $\delta^{13}C = \left[\frac{\left(^{13}C/^{12}C\right)}{\left(^{13}C/^{12}C\right)_{std}} - 1\right]1000‰$ can be used to estimate terrestrial carbon sources and sinks and their variability by solving for the respective atmospheric budget equations [e.g., *Keeling et al.*, 1989; *Francey et al.*, 1995; *Ciais et al.*, 1995; *Rayner et al.*, 1999; *Morimoto et al.*, 2000]. In particular, the 'double deconvolution' method distinguishes between ocean and land fluxes, because of the differences in isotopic fractionation between terrestrial-atmosphere and ocean-atmosphere fluxes. Therefore the assumed isotopic signature of terrestrial carbon fluxes is, among others, one of the sensitive variables in this method.

[4] Due to the heterogeneity and complexity of land ecosystems the terrestrial $^{13}CO_2$ flux field is highly variable in space and time. $^{13}C$ fractionation during photosynthesis depends on both climatic conditions [*Scholze et al.*, 2003; *Ito*, 2003] and vegetation composition ($C_4$ plants fractionate $^{13}C$ to a much smaller extent than $C_3$ plants) [*Craig*, 1954]. The $\delta^{13}C$ value of respired $CO_2$ can also be offset by a trend in atmospheric $\delta^{13}C$ since the respired carbon may have been fixed when the $\delta^{13}C$ was different from (older than) the current atmosphere. Hence there can be a net $^{13}CO_2$ flux without a net $CO_2$ flux due to the dilution of atmospheric $^{13}CO_2$ by fossil fuel combustion. This isotopic disequilibrium flux is a function of both the rate of change in atmospheric $\delta^{13}C$ and the residence times of carbon in terrestrial ecosystems. Therefore the $^{13}CO_2$ flux field of

[1]Max Planck Institut für Meteorologie, Hamburg, Germany.
[2]Now at QUEST - Department of Earth Sciences, University of Bristol, Bristol, UK.
[3]Laboratoire des Sciences du Climat et de l'Environment, Gif sur Yvette, France.
[4]Max-Planck-Institut für Biogeochemie, Jena, Germany.


0886-6236/08/2006GB002899$12.00

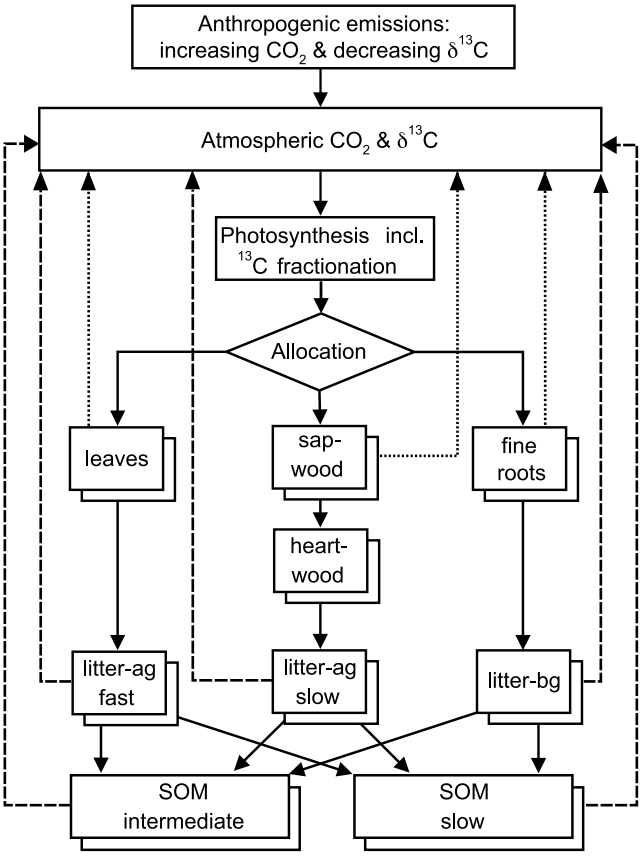


**Figure 1.** Carbon cycling within LPJ: all carbon pools are doubled with respect to $^{13}$C, autotrophic respiration (dotted arrows) is assumed to have the same isotopic signature as the photosynthate, while heterotrophic respiration (dashed arrows) is in disequilibrium with carbon uptake.

the land biosphere is affected by various quantities, e.g., atmospheric $\delta^{13}$C trend, the turnover times distribution of decomposing organic matter, vegetation composition, and climate [*Battle et al.*, 2000]. The use of atmospheric $CO_2$ and $\delta^{13}$C to study the global carbon cycle depends upon both various, accurate measurements of atmospheric $\delta^{13}$C and the application of models to characterize the terrestrial carbon isotope discrimination and the disequilibrium flux in space and time.

[5] Several process-based terrestrial biosphere models have calculated the spatial and seasonal patterns in terrestrial $^{13}$C discrimination [*Fung et al.*, 2003; *Wittenberg and Esser*, 1997; *Kaplan et al.*, 2002]. Recently, three model studies also analyzed the impact of climate variability on the $^{13}$C fractionation during photosynthesis [*Ito*, 2003; *Scholze et al.*, 2003; *Suits et al.*, 2005]. Land use, especially the conversion of forests into $C_4$ pastures in the tropics, has also been shown to effect the biosphere-atmosphere $\delta^{13}$C exchange and therefore, implies a change in the tropical land/ocean carbon sink distribution [*Townsend et al.*, 2002].

[6] Here, the study by *Scholze et al.* [2003] is extended using the isotope version of the Lund-Potsdam-Jena (LPJ) dynamic global vegetation model to investigate the impact of fire disturbance, and land use change in addition to the effects of climate on the terrestrial carbon isotope discrimination and isotopic disequilibrium in a consistent terrestrial carbon cycle modeling framework. The outline of this paper is as follows: In Section 2 we give a brief description of the model and the simulation experiments. Model validation and results from the experiments are shown and discussed in Section 3. A summary and conclusion is given in the last Section 4.

## 2. Methodology

### 2.1. The Lund-Potsdam-Jena Dynamic Global Vegetation Model

[7] Reported results are based on simulations using the LPJ dynamic global vegetation model [*Sitch et al.*, 2003]. The version of LPJ used here includes terrestrial carbon isotope discrimination. A description of the carbon isotope module within LPJ is given by *Scholze et al.* [2003]. Only the main features and the experimental set-up are described.

[8] LPJ combines the simulation of vegetation function (energy absorption, carbon and water cycling calculated daily) and structure (vegetation composition and biomass updated annually). Vegetation composition is described by nine plant functional types (PFT) which are distinguished according to their physiological ($C_3$, $C_4$ photosynthesis), morphological (tree, grass), phenological (deciduous, evergreen) and bioclimatic (heat/cold tolerance) attributes.

[9] Vegetation dynamics depends on disturbance, mortality, and establishment, but also on the productivity of the different PFTs. Ecosystem disturbance is modeled as fire events which are calculated based on litter moisture content, a fuel load threshold, and PFT specific fire resistances [*Thonicke et al.*, 2001]. Terrestrial carbon is represented by living tissue (leaves, sapwood, heartwood, and fine-roots), litter (above ground fast and slow, below ground) and soil (intermediate and slow) carbon. The fast and slow litter and the intermediate and slow soil pools are assigned turnover times at 10° C of 2, 20, 33, and 1000 years, respectively. Decomposition rates are soil moisture and soil temperature dependant [*Foley*, 1995; *Lloyd and Taylor*, 1994].

[10] Isotopic discrimination during $CO_2$ photosynthesis is calculated following *Lloyd and Farquhar* [1994] as a daily average value and depends mainly on the inter-cellular-to-atmospheric $CO_2$ concentration ratio, which is explicitly calculated by the LPJ photosynthesis equations. Gross photosynthesis and autotrophic respiration are assumed to be in isotopic equilibrium on timescales (seasonal and longer) relevant for this study [*Ekblad and Högberg*, 2001; *Bowling et al.*, 1999]. All internal carbon pools and mass fluxes between these pools are 'doubled' to keep track of $^{12}$C and $^{13}$C separately. As isotope fractionation processes during allocation, decomposition and respiration are poorly understood, no fractionations are assigned for these processes. The carbon isotope module used here is based on *Kaplan et al.* [2002] which has been compared with measurements of the land-atmosphere isotopic fractionation factors at various scales (leaf, canopy, and background atmosphere), therefore model results are only briefly compared to measurements. A sketch of the carbon cycling within LPJ is given in Figure 1.

**Table 1.** Performed LPJ Experiments and Prescribed Input Data

| Experiment | Prescribed |
|---|---|
| ISOVAR | atm. $CO_2$ $\delta^{13}C$, climate |
| ISOFIX | atm. $CO_2$ $\delta^{13}C$, climate, time invariant fractionation factor |
| ISOLU | atm. $CO_2$ $\delta^{13}C$, climate, land use, no pastures |
| ISOLUC | atm. $CO_2$ $\delta^{13}C$, climate, land use incl. $C_4$ crops, no pastures |
| ISOLUCP | atm. $CO_2$ $\delta^{13}C$, climate, land use incl. $C_4$ crops $C_4$ pastures |

[11] In addition to the two simulation experiments described by *Scholze et al.* [2003] (ISOVAR and ISOFIX) with respectively calculated or prescribed $C_3$ and $C_4$ plant distribution and leaf discrimination values, three more simulation experiments are performed (see Table 1). All experiments are calculated on a 0.5° spatial resolution using the CRU05 1901–1998 monthly climate (temperature, precipitation and cloud cover) time-series [*New et al.*, 2000], which are interpolated to daily values within LPJ. The time series of atmospheric $CO_2$ as described by *McGuire et al.* [2001] and an extended version of the atmospheric $\delta^{13}C$ time series of *Francey et al.* [1999] are used as further input data in all experiments. In the ISOVAR, ISOLU, ISOLUC, and ISOLUCP experiments the $^{13}C$ fractionation factor is calculated according to the *Lloyd and Farquhar* [1994] scheme as described above, while for the ISOFIX experiment a constant fractionation factor of −18.7‰ for $C_3$ plants and −4.9 for $C_4$ plants (global mean values from the ISOVAR experiment) is prescribed. For all experiments, reported isotopic values are calculated as flux-weighted sums first over time and second over space if applicable.

### 2.2. Land Use Change Scheme

[12] The ISOLU simulation follows the land use scheme developed by *McGuire et al.* [2001]. This land use scheme includes the 1) conversion from natural vegetation to cultivation, 2) production and harvest at cultivated sites, 3) the abandonment of cultivated sites, and 4) the decay of harvested wood products in different pools outside ecosystems. The flux associated with the conversion is simulated as a release of $CO_2$ due to the clearing (burning of slash, fuelwood). Harvested biomass from cultivated sites is decayed to the atmosphere from three product pools with different residence times based on their uses: 1 year (agricultural products), 10 years (paper products), and 100 years (lumber products). If a previously cultivated site has been abandoned the model is allowed to grow back natural vegetation and biomass from the current state at the time of abandonment. Regrowing vegetation is calculated by LPJ as either $C_3$ or $C_4$ plants depending on the local climate conditions. The locations of cultivated sites and their conversion and abandonment years are derived from the historical (1700 to 1992) fractional croplands data set of *Ramankutty and Foley* [1999] which has been transformed to a boolean croplands data set preserving total cropland area at a 5° gridcell level. Thus a 0.5° model gridcell is either treated as being agricultural or natural but keeping the vegetation cover as simulated by LPJ. Between 1993 and 1998 the cropland area of 1992 has been used. The net primary productivity (NPP) of cultivated sites is estimated using the relative agricultural productivity (RAP) approach [*Esser*, 1995]. The RAP data set defines the agricultural productivity relative to the productivity of the natural vegetation on a country specific basis. Therefore no changes are made to the simulated vegetation cover.

[13] In addition to the general land use scheme applied in the ISOLU simulation, the temporal and spatial extent of $C_4$ crops (corn, sugar cane, millet, and sorghum) has been prescribed in the ISOLUC experiment in order to calculate the influence of $C_4$ crops on the terrestrial isotopic signature. A country specific data set of the area covered with $C_4$ crops has been compiled from the *FAO* [2002] database for the years 1961 to 1998. This area in each country is then transformed into a fraction covered by $C_4$ crops of a 0.5° gridcell by dividing the $C_4$ crop area with the total crop area given by *Ramankutty and Foley* [1999] for each country using a gridded (0.5° resolution) political map of the world. In a very few cases (less than 1% of the 0.5° gridcells covered with $C_4$ crops) the $C_4$ crop fraction is greater than one because the *Ramankutty and Foley* [1999] global data set contains less area covered by all crops than the area of $C_4$ crops present in the *FAO* [2002] inventory statistics (e.g., gridcells located in Eritrea, Congo or Benin). In these cases the $C_4$ crop fraction is then set to one. The mean ratio over the years 1961 to 1970 of $C_4$ crop area to total crop area per country has been used to calculate the fractional $C_4$ crop

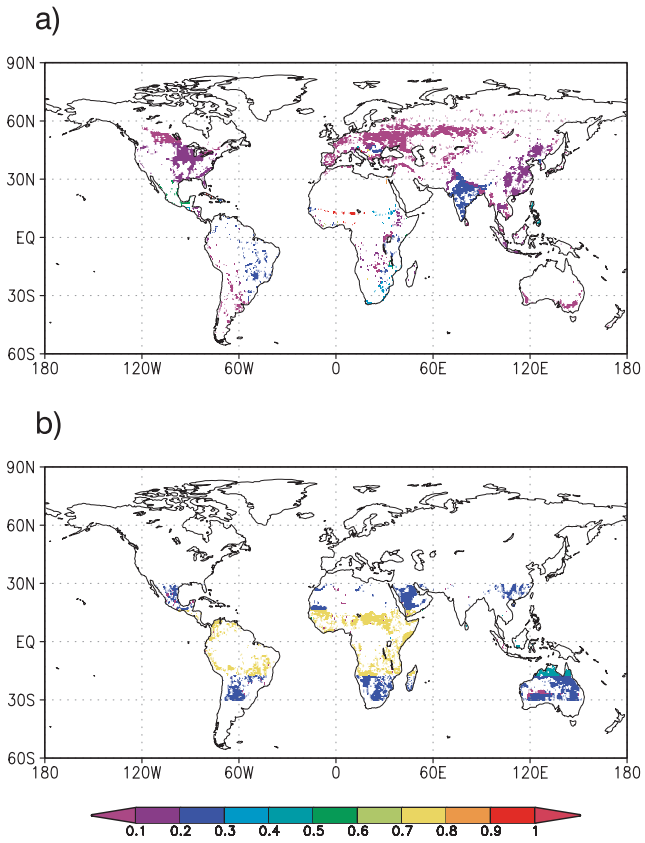


**Figure 2.** Spatial distribution of $C_4$ crops (a) and $C_4$ pastures (b) for the year 1990 (units are covered fraction of a gridcell).

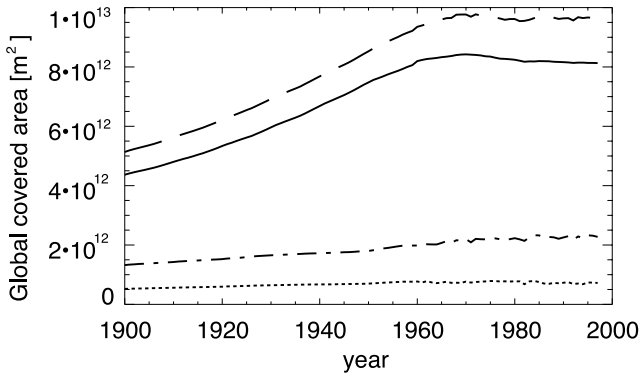


**Figure 3.** Time series of the global covered area with $C_4$ pastures (solid line) and $C_4$ crops (dashed-dotted line) as well as global covered area with $C_4$ land use in the wider Tropics (30°S to 30°N; dashed line) and for the land area north of 30°N (dotted line).

coverage for the years 1901 to 1960 using the *Ramankutty and Foley* [1999] data set. Figure 2 displays a snapshot of $C_4$ crop extent in the year 1990 and Figure 3 shows the time series of the global area covered by $C_4$ crops. A similar map of $C_4$ vegetation including also the global $C_4$ crop distribution has been compiled by *Still et al.* [2003]. However, their map represents a static picture of the $C_4$ vegetation distribution representative for the 1980s and 1990s, whereas for this study the temporal evolution is of importance.

[14] To analyze the impact of expanding tropical $C_4$ pastures on regional ecosystem isotope discrimination, tropical $C_4$ pastures as well as the above described $C_4$ crops have been specified in the ISOLUCP simulation. Global pasture area extent from 1700 to 1990 is taken from the HYDE database [*Klein Goldewijk*, 2001; *Klein Goldewijk and Battjes*, 1997] with a 0.5° spatial and 10 year temporal resolution. This data set has been linearly interpolated between the 10 year steps to obtain a pasture data set on a yearly time basis. In addition to the HYDE data, global pasture area per country from the *FAO* [2002] database covering the period 1961 to 1998 has been spatialized on a 0.5° grid using the same method as described above for the $C_4$ crops with the pasture maps from the HYDE database and keeping the spatial distribution constant after 1990. The amount of $C_4$ plants in tropical pastures is specified by *Townsend et al.* [2002] to be able to compare the disequilibrium fluxes due to $C_3$ to $C_4$ plant conversion: 80% of the pasture area is covered by $C_4$ plants in a zonal band from 17° S to 17° N in South America and Africa while only a value of 50% is assumed in this zonal band in Asia due to rice cultivation. In the area covered in the latitudinal band from 30° S to 17° S and 17° N to 30° N 30% of the pasture area is assumed to be covered by $C_4$ plants; south of 30° S and north of 30° N pastures are dominated by $C_3$ plants. A snapshot of the $C_4$ pasture extent from the year 1990 is shown in Figure 2 and the time series of the global area covered by $C_4$ pastures in Figure 3.

[15] In order to simulate $C_4$ land use in LPJ the fraction of the gridcell covered by $C_4$ crops and $C_4$ pastures is modeled using the $C_4$ grass PFT; in the remaining area of the gridcell LPJ simulates its own vegetation composition based on competition and the bioclimatic limits of the PFTs. Carbon 13 is treated the same way as total carbon in gridcells affected by a change in land use, i.e., for each of the three total carbon land use product pool exists a respective $^{13}$C pool for separate accounting.

### 2.3. Isotopic Disequilibrium

[16] The isotopic disequilibrium flux from the terrestrial biosphere is given by [e.g., *Joos and Bruno*, 1998]

$$D_{\mathrm{b}} = F_{\mathrm{ba}}[\delta^{13}C_{\mathrm{resp}} - (\delta^{13}C_{\mathrm{a}} + \epsilon_{\mathrm{ab}})] \quad (1)$$

where $F_{\mathrm{ba}}$ is the $CO_2$ flux from the land biosphere to the atmosphere (ecosystem respiration $R_{\mathrm{eco}}$ which is the sum of the modeled autotrophic respiration, heterotrophic respiration, fire emission and in case of the land use experiments also include the wood and food products decay emission), and $\delta^{13}C_{\mathrm{resp}}$ is the resulting isotopic ratio of this flux. $\delta^{13}$Ca is the isotopic ratio of atmospheric $CO_2$ and $\epsilon_{\mathrm{ab}}$ the fractionation factor during $CO_2$ assimilation. The isotopic disequilibrium is then given by the difference between the isotopic ratios of the uptake flux and of the ecosystem respiration:

$$D_b = (\delta^{13}C_{\mathrm{resp}} - (\delta^{13}C_{\mathrm{a}} + \epsilon_{\mathrm{ab}})) = \delta^{13}C_{\mathrm{resp}} - \delta^{13}C_{\mathrm{leaf}} \quad (2)$$

Major controls on the disequilibrium are therefore interannual variability in leaf discrimination due to climate variability and changes in vegetation composition or variability in the isotopic ratio of ecosystem respiration due to changes in the carbon residence time. The carbon residence time in the natural vegetation simulations (ISOVAR) is mainly regulated by climate (temperature dependence of the respiration fluxes) and ecosystem disturbance (wildfires). In the land use experiments the residence time is also altered by the decay of the product pools and by the conversion from natural vegetation to cultivation, respectively.

[17] Fire emissions are calculated from the burnt biomass of leaf foliage, woody tissue and the aboveground litter pool. The isotopic signature of the biomass burning is computed as the flux-weighted mean of the isotopic ratios of the respective pools. In the LPJ model calculation the average carbon content in these pools is younger than the carbon of the soil pools in the sense of the time elapsed since assimilation. This ignores sporadic burning of very old carbon stocks, such as the peat forest fires in Indonesia during 1997–1998 [*Page et al.*, 2002]. Because of the change in $\delta^{13}C_{\mathrm{a}}$ from fossil fuel burning the fire flux is therefore more depleted in $^{13}$C than the heterotrophic respiration flux and thus, reduces the isotopic disequilibrium. To quantify the influence of the fire flux on the isotopic disequilibrium, $\delta^{13}C_{\mathrm{resp}}$ is calculated by replacing the isotopic signature of the fire flux, $\delta^{13}C_{\mathrm{fire}}$, with the isotopic signature of heterotrophic respiration, $\delta^{13}C_{R_{\mathrm{h}}}$. In this sensitivity experiment the amount of the total ecosystem respiration flux is not changed by assuming that the missing biomass burning flux is compensated by an increased heterotrophic respiration. It determines, however, a

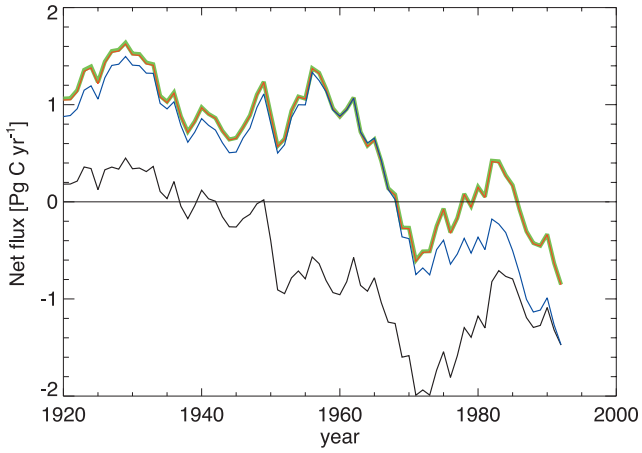


**Figure 4.** Simulated 10-year running means of the global terrestrial net carbon exchange between 1920 and 1992 (positive values indicate net release to the atmosphere). Colors represent: green ISOLU, red ISOLUC, blue ISOLUCP and black ISOVAR.

shift in the isotopic signature of the ecosystem respiration as $\delta^{13}C_{fire}$ and $\delta^{13}C_{R_h}$ usually have different values. These results are purely diagnostic and denoted under the 'ISOVAR without fire' experiment.

## 3. Results and Discussion

### 3.1. Net Terrestrial Carbon Fluxes

[18] Net carbon exchange (NCE) is defined as in *McGuire et al.* [2001]:

$$NCE = R_h + F_{fire} - NPP \quad (3)$$

or in the case of the land use experiments as:

$$NCE = R_h + F_{fire} + F_{prod} + F_{conv} - NPP \quad (4)$$

A positive NCE indicates a terrestrial source of atmospheric $CO_2$, whereas a negative NCE indicates a terrestrial sink. The total terrestrial net carbon fluxes as simulated by the ISOVAR and ISOLU experiment have already been discussed in detail by *McGuire et al.* [2001] (the ISOVAR experiment corresponds to their S2 simulation and the ISOLU experiment to their S3 simulation). Results of the net fluxes presented here are slightly different than the values reported by *McGuire et al.* [2001] as the climate input data are not exactly the same. In Figure 4 smoothed global records of net carbon exchanges for the different experiments from this study are shown. As already discussed by *McGuire et al.* [2001] the net carbon exchange substantially changed from neutral (ISOVAR) or release (ISOLU, ISOLUC, ISOLUCP experiments) to storage of carbon after 1970. The storage seems to be associated with both the $CO_2$ fertilization effect (as seen in the ISOVAR experiment) and for the land use experiments also with the deceleration in the expansion of croplands and therefore the decline in the $CO_2$ release from land use conversion which peaked around 1950. This is specific to the data set used here [*Ramankutty and Foley*, 1999] whereas the data set by *Houghton* [2003] gives a stable rate of cropland expansion after 1950.

[19] The effect of land use on the total ($^{12}C$ + $^{13}C$) terrestrial carbon budget results into a flux of 0.96 Pg C yr$^{-1}$ to the atmosphere over the years 1980 to 1989 (mean net carbon exchange of −0.7 Pg C yr$^{-1}$ (flux to the biosphere) for the ISOVAR experiment compared to 0.26 Pg C yr$^{-1}$ for the ISOLU experiment). Adding $C_4$ crops to the land use scheme (ISOLUC simulation, mean net carbon exchange of 0.25 Pg C yr$^{-1}$ over the years 1980 to 1989) does not change the terrestrial carbon budget as compared to the ISOLU experiment. However, including tropical $C_4$ pastures (ISOLUCP) gives a total net carbon exchange of −0.4 Pg C yr$^{-1}$ for this time period. The larger flux to the biosphere in the ISOLUCP experiment compared to the ISOLUC experiment in Figure 4 is mainly apparent in the years from 1970 until 1998. In the years preceding this period, there is almost no difference to the ISOLU and ISOLUC experiment. Figure 4 shows that from 1970 onwards the global area of tropical $C_4$ pastures decreases slightly as former grazing areas are abandoned to regrowing forests leads to an additional terrestrial carbon storage.

### 3.2. Discrimination During Photosynthesis

#### 3.2.1. Comparison With Measurements

[20] Monthly mean $^{13}C$ discrimination values at the leaf level (denoted as $\Delta_{leaf}$) during photosynthesis from the ISOVAR simulation can be compared with measurements of leaf discrimination (data compiled by *Buchmann and Kaplan* [2001]) at PFT level. Agreement between simulated and measured values is good: results correspond for almost all PFTs within one standard deviation (≈2‰). Variations in $\Delta_{leaf}$ among the $C_3$ PFTs is of the order of 6‰ for the simulated and slightly less for the measured values. This variability reflects both the diversity in discrimination among different plant types and the response of $^{13}C$ discrimination to interannual climate variability and is well captured by LPJ.

#### 3.2.2. Impact of Land Use on Leaf Discrimination

[21] There is almost no difference in the spatial distribution of mean (1985 to 1995) annual leaf discrimination, $\Delta_{leaf}$, between the experiment with potential natural vegetation (ISOVAR) and the land use experiment (ISOLU, not shown). The spatial heterogeneity in $\Delta_{leaf}$ in the ISOVAR simulation reflects the effect of arid environments and PFT distribution (Figure 5a); lowest values in discrimination occur in very dry climatic regions (e.g., Central Asia) or in regions with a high amount of $C_4$ plants (Brazilian grasslands, subtropical Africa and northern Australia). High leaf discrimination values can be found in very humid environments such as the tropical rain forest or regions with low light intensity that limits photosynthetic rates such as the boreal forest. In contrast to the natural vegetation, the spatial distribution of $\Delta_{leaf}$ for land use vegetation shows the importance of specifying $C_4$ crops (the North American corn belt, south eastern Europe, the Indian subcontinent and Southeast Asia, Figure 5b) and $C_4$ pastures (South America, Africa and also Australia, Figure 5c) especially in regions where the natural vegetation is forest. However, somehow

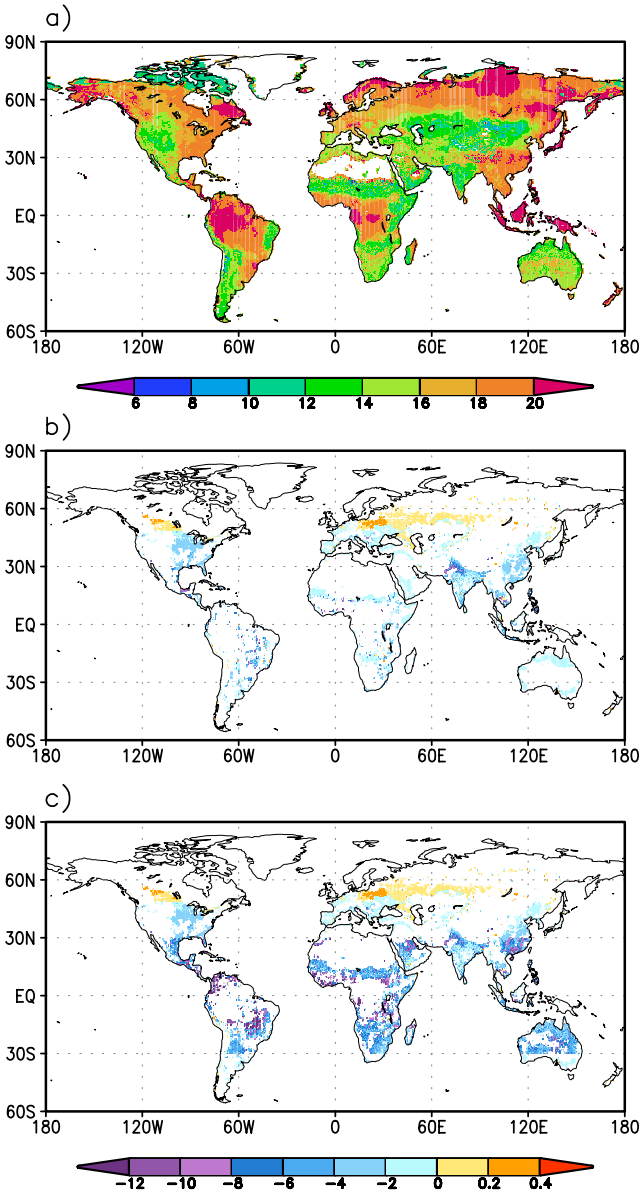


**Figure 5.** Mean modeled annual leaf discrimination over the years 1985 to 1995 for (a) potential natural vegetation (ISOVAR), and difference between (b) vegetation including $C_4$ crops (ISOLUC-ISOVAR), and (c) vegetation including $C_4$ crps and $C_4$ pastures (ISOLUCP−ISOVAR) and potential natural vegetation. Units are ‰.

counter-intuitive are the slightly higher discrimination values in the ISOLUC and ISOLUCP experiments for the Canadian prairie region and for East Europe and parts of Russia (see Figure 5). In these temperate grassland areas LPJ simulates an overabundance of trees, which is especially pronounced if only a small fraction of a grid-cell (less than 0.1, see Figure 2) is specified as covered with $C_4$ crops. The remaining grid-cell then is almost fully covered with $C_3$ forest leading to higher discrimination values. An additional effect is that with some fraction of a grid-cell specified as $C_4$ crops there is less competition among the $C_3$ trees for soil water, and thus a higher $C_3$ photosynthetic rate. This is because in LPJ different PFTs in the same gridcell share the same soil water reservoir. $C_4$ crops (represented as the $C_4$ grass PFT in the model) can only access soil water from the first soil layer, whereas $C_3$ trees have deeper roots and can also extract water from the second soil layer. The overall increase in the $C_3$ productivity is higher than what is substituted for with the $C_4$ crops.

[22] Globally flux-weighted annual leaf discrimination averaged over the years 1982 to 1992 varies between 17.58‰ for the ISOVAR experiment and 17.04‰ for the ISOLUCP experiment (see Table 2), a reduction of more than 0.5‰ in the global value because of $C_4$ land use. Yet because we use the NPP of $C_4$ grasses for $C_4$ crops, and ignore the fertilization of pastures by grazing animals, it is likely that our simulated NPP of $C_4$ cultivated lands with a mean estimate of 3.5 (3.2 for $C_4$ pastures and 0.3 for $C_4$ crops) Pg C $yr^{-1}$ over the years 1982 to 1992 is lower than in reality. This would cause a systematic underestimate in $\Delta_{leaf}$ in ISOLUCP. Our $\Delta_{leaf}$ values lie well within the range of values from other studies: 14.8‰ [*Lloyd and Farquhar*, 1994] to 18.2‰ [*Ito*, 2003]. *Lloyd and Farquhar* [1994] probably over-emphasize the importance of $C_4$ photosynthesis and report therefore the lowest discrimination value. *Still et al.* [2003] found a global discrimination value of 16.5‰ considering also $C_4$ crops which is less than the 17.07‰ from the ISOLUCP simulation. *Kaplan et al.* [2002] (18.6‰) and *Bakwin et al.* [1998] (16.8‰) report global ecosystem discrimination (see Equation 5) values which are comparable to 17.8‰ from the ISOVAR experiment.

[23] The impact of a climate-dependent discrimination during $CO_2$ assimilation on inverse methods to quantify terrestrial carbon fluxes has already been discussed by *Scholze et al.* [2003]. The interannual variability in the ISOFIX experiment is reduced by approximately a factor of three as compared to the ISOVAR simulation. Also, the long-term trend in discrimination in the ISOVAR experiment (an increase of about 0.4‰, see Figure 6) has already been noted by *Scholze et al.* [2003] to be a

**Table 2.** Simulated Mean Global Flux-Weighted Leaf Discrimination, Isotopic Disequilibrium $\mathcal{D}_b$, Isotopic disequilibrium Flux $D_b$, and Total Ecosystem Respiration Flux $F_{resp}$ Which is the sum of Heterotrophic Respiration and Fire Flux or in the Case of the Land use Experiments the sum of Heterotrophic Respiration, Fire, Conversion and Agricultural Productivity Flux for the Period 1982–1992[a]

| Experiment | $\Delta_{leaf}$ [‰] | $\mathcal{D}_b$ [‰] | $D_b$ [Pg C ‰ $yr^{-1}$] | $F_{resp}$ [Pg C $yr^{-1}$] |
|---|---|---|---|---|
| ISOVAR | 17.58 | 0.49 | 34.8 | 69.4 |
| ISOVAR without fire | | 0.63 | 44.7 | 69.4 |
| ISOFIX | 17.93 | 0.45 | 31.5 | 69.4 |
| ISOLU | 17.58 | 0.46 | 29.1 | 64.3 |
| ISOLUC | 17.42 | 0.41 | 28.5 | 64.5 |
| ISOLUCP | 17.04 | 0.35 | 20.7 | 62.7 |

[a]The isotopic disequilibrium values for the ISOVAR without fire row are purely diagnostics and as fire has no influence on the leaf discrimination no values are diagnosed.

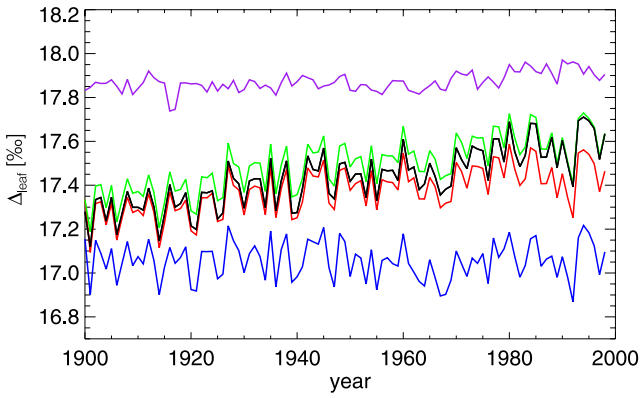


**Figure 6.** Time series of modeled carbon isotope discrimination $\Delta_{leaf}$. Colors represent: purple ISOFIX, green ISOLU, black ISOVAR, red ISOLUC and blue ISOLUCP.

response to climate. A review of tree ring cellulose $^{13}$C studies showed that there is no general pattern of discrimination; values either increased, decreased or remained constant during the recent past [*Arneth et al.*, 2002; *Bert et al.*, 1997; *Duquesnay et al.*, 1998; *Hemming et al.*, 1998; *Leavitt and Lara*, 1994; *Marshall and Monserud*, 1996; *Raffalli-Delerce et al.*, 2004]. This reflects the site specific environmental conditions for tree growth, and thus, renders a direct comparison between large scale model results and site specific tree ring isotope values difficult.

[24] As can be seen from Figure 6, the magnitude and pattern of interannual variability in the flux-weighted global leaf discrimination does not change significantly in the land use experiments as compared to the ISOVAR experiment. However, the total magnitude of the discrimination is reduced substantially in the ISOLUCP experiments with prescribed $C_4$ crops and $C_4$ pastures. Also, for the ISOLUCP experiment there is no trend in the discrimination for the years 1900 to 1960 as compared to the ISOVAR, ISOLU and ISOLUC experiments because of the counteracting effect of the highly increasing amount of $C_4$ pastures until 1960 (see Figure 3). The different value in 1900 for the ISOLUCP experiment compared to the other experiments is because the $C_4$ pasture area has been specified from 1700 onwards whereas the $C_4$ crop area has only been specified from 1901 onwards. The long-term increasing trend which is apparent in the ISOVAR, ISOLU and ISOLUC simulations is due to climatic effects [*Scholze et al.*, 2003]. The specification of $C_4$ crops alone seem to compensate for the climate induced rising trend in $\Delta_{leaf}$ after 1970. The additional specification of $C_4$ pastures in the ISOLUCP simulation seems to compensate this trend over the whole last century by the higher amount of low $C_4$ plant discrimination values.

#### 3.2.3. Mapping the Temporal Variability of Leaf Discrimination

[25] The standard deviation of the spatially explicit modeled discrimination illustrates areas with high temporal variability in the discrimination. In order to account for areas with high variability in the fractionation factor due to changes in the presence and non-presence of PFTs in these regions (e.g., borders of deserts where gross $CO_2$ fluxes are also small), Figure 7 shows the product of the standard deviation of $\Delta_{leaf}(t)$ with the mean NPP for the years 1950 to 1998. The displayed quantity is the standard deviation of an isoflux, but only with the variability of the discrimination contributing to it. Figure 7a displays this quantity for the ISOVAR experiment. Areas with high values in Figure 7a such as Central America, the subtropics in Africa, India, and parts of Southeast Asia are the transition zones between tropical and subtropical climate. Variability there is mainly due to the interannual variations in the $C_3/C_4$ plant distribution and thus in the relative amount of $C_4$ productivity compared to $C_3$ productivity per gridcell. Figure 7b shows the difference between the ISOVAR and ISOFIX experiment in the standard deviation of this isoflux. The difference reveals the regions where the variability is caused solely by variations in the fractionation factor of $C_3$ plants imposed by climate variability. The dominant areas here are mainly the temperate zones (North America, Europe, eastern Asia) and parts of the tropics. Figure 7b also reveals regions where the standard deviation of this isoflux is similar between ISOVAR and ISOFIX, i.e., the lowest values in Figure 7b. These areas are in the tropicssubtropics, e.g., sub-saharan Africa, which is dominated by savannah vegetation (mainly a mixture of deciduous trees and $C_4$ grass). This is consistent with the low variance in modeled leaf discrimination there for tropical PFTs, and with the high variance in the $C_3$ versus $C_4$ annual share of NPP. However, as the measured variance for tropical PFTs is much higher, it seems that the sensitivity of the $^{13}$C discrimination during photosynthesis against climate is underestimated for the tropical PFTs in the model.

### 3.3. Ecosystem Discrimination and Isotopic Disequilibrium

#### 3.3.1. Comparison With Measurements

[26] Ecosystem discrimination, ($\Delta_e$), is an integrated signal of the $^{13}$C signature of ecosystem $CO_2$ exchange with the atmosphere (see *Buchmann et al.* [1998] for the concept of ecosystem discrimination). Modeled ecosystem discrimination is calculated as the flux weighted difference (respecting the sign of the fluxes) in isotopic discrimination from NPP and ecosystem respiration ($R_{eco}$, again $R_{eco}$ does not include autotrophic respiration here):

$$\Delta_e = \frac{\Delta_{leaf} NPP - \Delta_{resp} R_{eco}}{NPP - R_{eco}} \quad (5)$$

Three major processes determine the value of $\Delta_e$: (1) plant available soil moisture, (2) photosynthesis rate and (3) the turnover time of soil carbon. Maximum flux-weighted zonal mean $\Delta_e$ values can be found close to the equatorial tropics and the boreal regions due to the high photosynthetic $^{13}$C discrimination values of tropical and boreal forests (Figure 8). The wide range of $\Delta_e$ values within areas dominated by $C_3$ vegetation (≈16‰ to 21‰) demonstrate the changing water availability for the plants and their adaptation to arid environments as well as the differences in soil carbon turnover time. The lowest modeled values can be found in the subtropics because of the relatively high amount of $C_4$ plants but also at latitudes around 40° N due to the rather

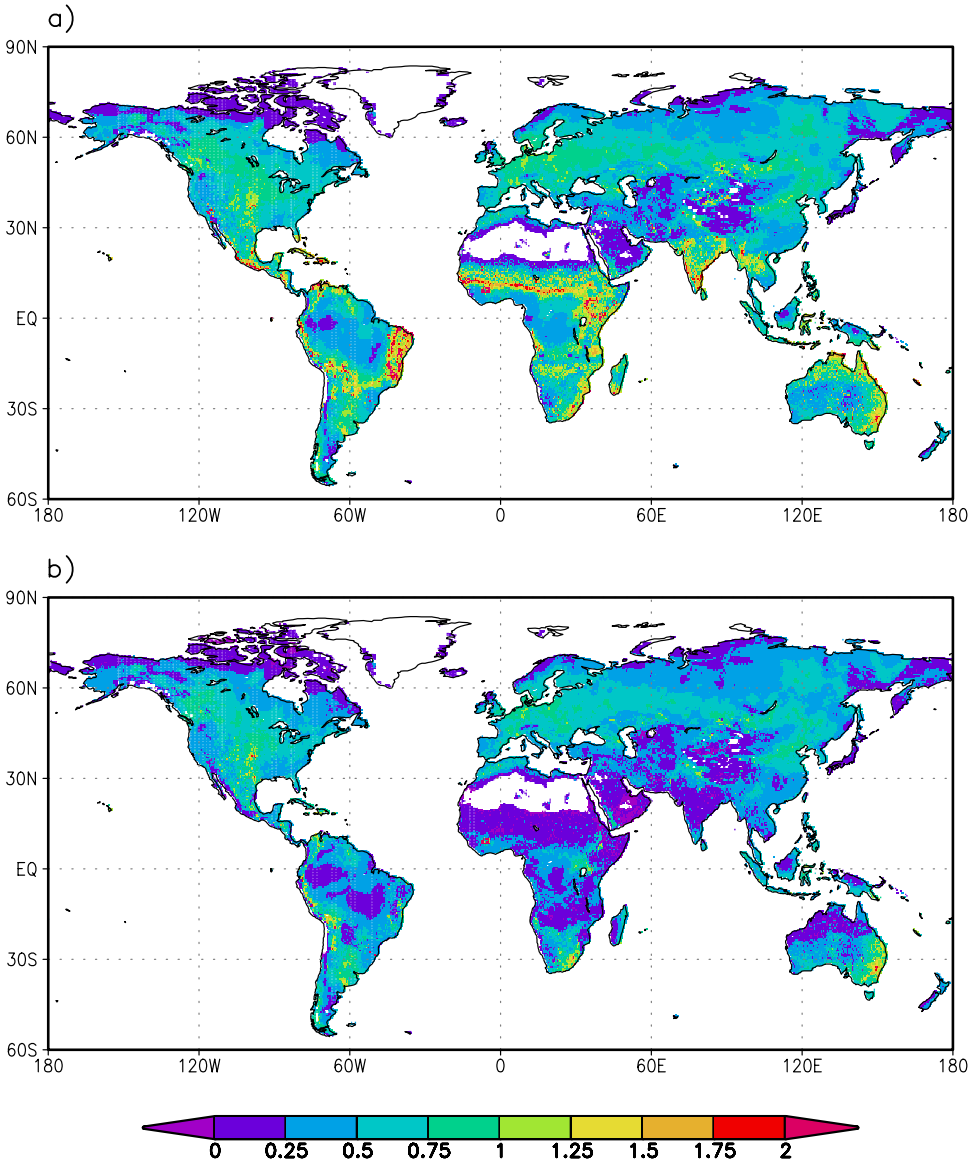


**Figure 7.** Interannual standard deviation of $\Delta_{leaf}$ leaf multiplied by the mean *NPP* over the past 30 years (similar to the standard deviation of an isoflux). (a) for the ISOVAR experiment and (b) for the difference between ISOVAR and ISOFIX. Units are kg C ‰ $m^{-2}$ $yr^{-1}$.

arid climate, which leads to a reduced transpiration of $C_3$ plants. Measurements of ecosystem discrimination of natural vegetation (data also compiled by *Buchmann and Kaplan* [2001]) agree well with the simulated values of $\Delta_e$ at various latitudes and are almost always lying within the range of one standard deviation in the temporal variations around the simulated mean.

### 3.3.2. Impact of Land Use on Ecosystem Discrimination

[27] The land use scheme without specifying $C_4$ crops and $C_4$ pastures (ISOLU simulation) has a negligible effect on the latitudinal variations in ecosystem discrimination (Figure 9). However, specifying $C_4$ crops (ISOLUC experiment) clearly reduces ecosystem discrimination in the northern hemisphere between 15° N to 50° N by about 1.5‰ (North American corn belt, European and Asian $C_4$ agriculture). The highest reduction of almost 3‰ in $\Delta_e$ occurs in a latitudinal band between 30° S and 17° S as modeled in the ISOLUCP experiment reflecting the influence of extensive grazing areas in South America, South Africa and Australia which were assumed to consist only of 30% $C_4$ plants. Although the specified fraction of $C_4$ pastures for the inner tropics (17° S to 17° N) is much higher than for the outer tropics (80% compared to 30%, see Figure 3), the reduction in ecosystem discrimination is significantly less (but still a reduction of ≈1‰ in $\Delta_e$) because of the higher discrimination values of the tropical forest PFTs and their greater productivity in comparison to the tropical $C_4$ pastures: mean NPP of 22.9 Pg C $yr^{-1}$ over

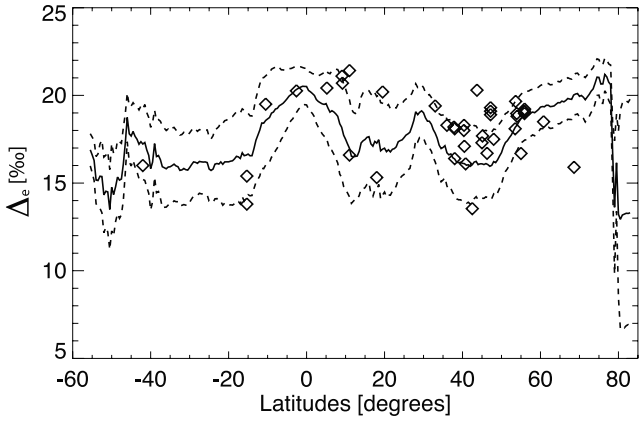


**Figure 8.** Simulated flux-weighted latitudinal ecosystem discrimination (line) from the ISOVAR simulation averaged over the years 1950 to 1998 and measured ecosystem discrimination (symbols). Dashed lines represent one temporal standard deviation around the simulated mean.

the years 1950–1998 for tropical forests compared to 2.7 Pg C yr$^{-1}$ for tropical $C_4$ pastures.

### 3.3.3. Modeled Isotopic Disequilibrium

[28] In all experiments, the average flux-weighted isotopic disequilibrium ($\mathcal{D}_b$) over the years 1985 to 1995 exhibits a high spatial variability (Figure 10a for the ISOVAR experiment). In general, $\mathcal{D}_b$ values are high, around 1‰ to 1.5‰, in regions where the turnover time of soil carbon is large (northern hemisphere boreal forests), whereas low $\mathcal{D}_b$ values, around 0‰, can be found in areas with a high amount of herbaceous vegetation as turnover times are usually shorter for grasslands than for forests. This is in agreement with the findings of *Fung et al.* [1997] and *Ciais et al.* [1997], they report low values of ≈0.2‰ for grasslands and deserts and high values of more than 0.5‰ for boreal forests.

[29] Fire has an important impact on the spatial pattern of the isotopic disequilibrium; regions where LPJ simulates a high fire frequency, usually dry areas with enough biomass to sustain frequent fires such as the American grasslands, subtropical Africa, parts of India and Australia, have a much lower (a difference of ≈1‰) isotopic disequilibrium in the ISOVAR simulation than in the ISOVAR without fire experiment (see Figure 10b for the difference between the ISOVAR simulation and ISOVAR without fire experiment). This confirms the fact that in LPJ carbon turnover time in ecosystems is shortened by fire events as compared to soil decomposition. Only natural fire events are modeled in LPJ, therefore areas with a high amount of anthropogenic biomass burning such as Southeast Asia are almost not affected. However, the effect of anthropogenic fires applied during deforestation actions is implicitly included in the calculation as part of the land use induced isotopic disequilibrium through the conversion flux.

[30] Both $C_4$ crops and $C_4$ pastures have a distinct influence on $\mathcal{D}_b$, especially in areas where forest is converted to $C_4$ crops or $C_4$ pastures. After the conversion the ecosystem respiration still carries the isotopic signal of the former $C_3$ forest whereas the assimilation flux has the much lower isotopic signature of newly established $C_4$ cultivation. Thus a recently cleared grazing or crop area has a negative disequilibrium value as compared to an old pasture where the $C_3$ fraction of ecosystem respiration has already declined (Figure 11). Low isotopic disequilibrium values (around 0‰) due to $C_4$ land use can be found in the North American corn belt established long ago, South American grazing areas (Brazil and Argentina), South Africa and in parts of Europe and Southeast Asia (Figures 10c and 10d for the differences between ISOVAR and ISOLUC and ISOLUCP, respectively).

[31] Mean modeled values of the global flux-weighted isotopic disequilibrium and the disequilibrium isoflux and the corresponding ecosystem respiration fluxes averaged over 1982–1992 are presented in Table 2. An increasing trend in $\mathcal{D}_b$ through time (see Figure 12) due to the change in the atmospheric isotopic ratio from intensified fossil fuel burning is clearly visible (0.34‰ for the period 1962–72 compared to 0.49‰ for the period 1982–92 as simulated in the ISOVAR experiment). These results lie well within values reported elsewhere (e.g., 0.56‰ by *Ciais et al.* [1999]), see Table 3 for a comparison with other studies. Furthermore, modeled global values of the isotopic disequilibrium differ considerably among the different experiments: while the ISOVAR without fire experiments yields the highest $\mathcal{D}_b$ mean value of 0.63‰ (for 1982–92), the ISOLUCP experiment estimates a mean value of only 0.35‰ for the same period. This decline in $\mathcal{D}_b$ is a result of several processes: first, $\delta^{13}$C values of fire emissions are closer to the isotopic composition of newly formed biomass than the $\delta^{13}$C values of respiratory soil emissions (see section 2) and second, the highly reduced discrimination during $C_4$ photosynthesis compared to $C_3$ photosynthesis over-compensates the decrease in atmospheric $\delta^{13}$C and therefore, largely reduces or even changes the sign in the difference of newly formed phytomass and ecosystem respiration at regions which have recently been converted

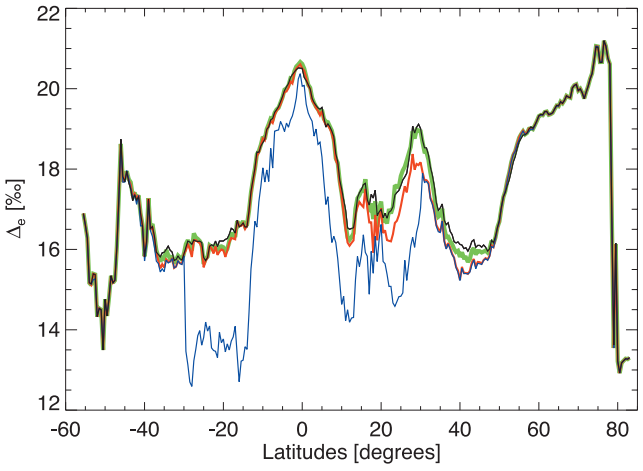


**Figure 9.** Simulated flux weighted latitudinal ecosystem discrimination averaged over the years 1950 to 1998. Colors represent: black ISOVAR, green ISOLU, red ISOLUC and blue ISOLUCP.

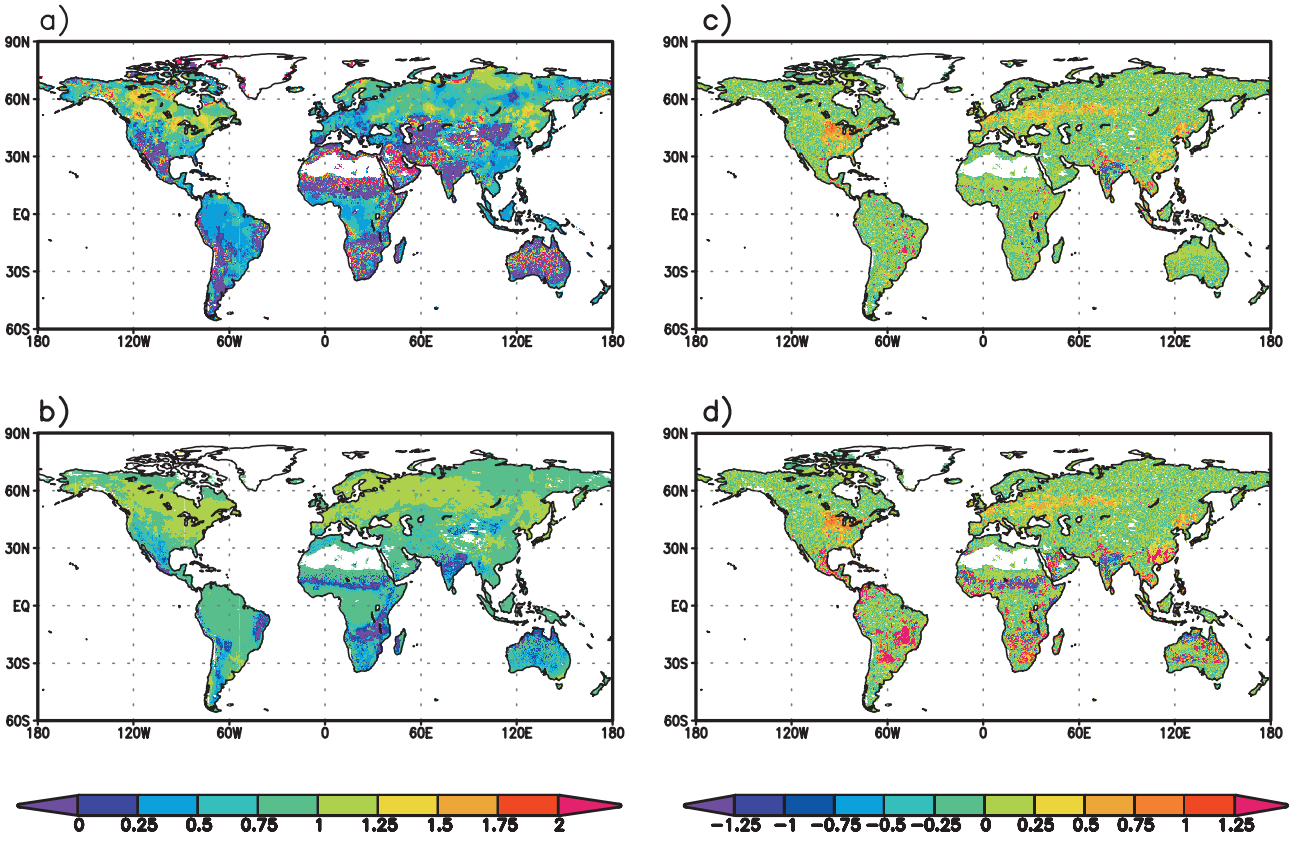


**Figure 10.** Spatial pattern of the mean flux-weighted isotopic disequilibrium over the years 1985 to 1995 for (a) ISOVAR (left color bar), the difference between ISOVAR and (b) ISOVAR without fire, (c) ISOLUC, and (d) ISOLUCP experiment (Figures 10b, 10c, and 10d right color bar). Units are ‰.

from $C_3$ plants to $C_4$ plants. Together with calculations of the ecosystem respiration, the global isotopic disequilibrium flux reported in Table 2 ranges from 44.7 Pg C‰ yr$^{-1}$ (ISOVAR without fire) to 20.7 Pg C‰ yr$^{-1}$ (ISOLUCP). This is partly due to the slightly reduced total ecosystem respiration flux (69.4 Pg C yr$^{-1}$ for the ISOVAR, ISOVAR without fire and ISOFIX experiments to 62.7 Pg C yr$^{-1}$ for the ISOLUCP experiment) but mainly because of the highly reduced $\mathcal{D}_b$: 0.63‰ (ISOVAR without fire) compared to 0.35‰ (ISOLUCP). The ISOVAR without fire calculations yield a 'real' (meaning an isoflux without a flux in total carbon) additional isotopic disequilibrium flux as the total respiration flux does not change in the calculations, however only the isotopic signature of the fire flux is changed (Section 2.3). The effect of fire is an overall reduction of the mean residence time of carbon as the occurrence of biomass burning bypasses the cycling of carbon through litter and soil carbon pools. Table 3 summarizes and compares results from this study with previous studies. In general, the agreement with values from previous studies is better with results from the ISOLUCP experiment than from the ISOVAR experiment.

[32] Partitioning the reduction in the global disequilibrium flux to the various processes reveals that the modeling of natural biomass burning reduces $D_b$ by around 10 Pg C‰ yr$^{-1}$. The total amount of simulated fire emissions is rela-

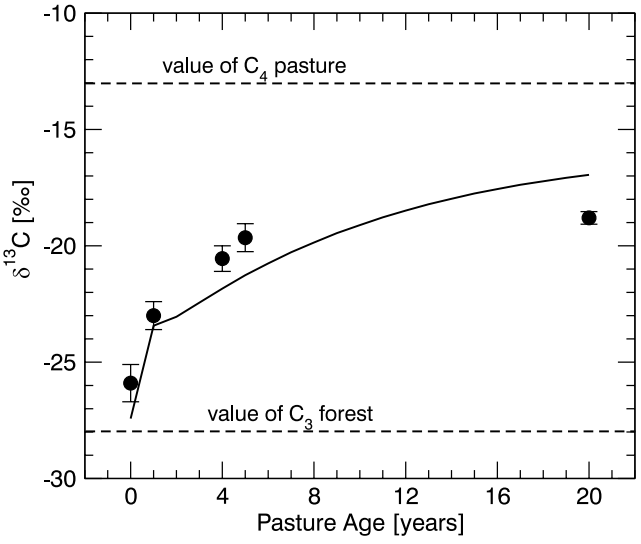


**Figure 11.** Modeled isotopic ratio of heterotrophic respiration after clearance of $C_3$ forest to $C_4$ pasture. Data points are from a field site in Costa Rica *Townsend et al.* [2002]. Note that the temporal resolution of modeled values is one year.

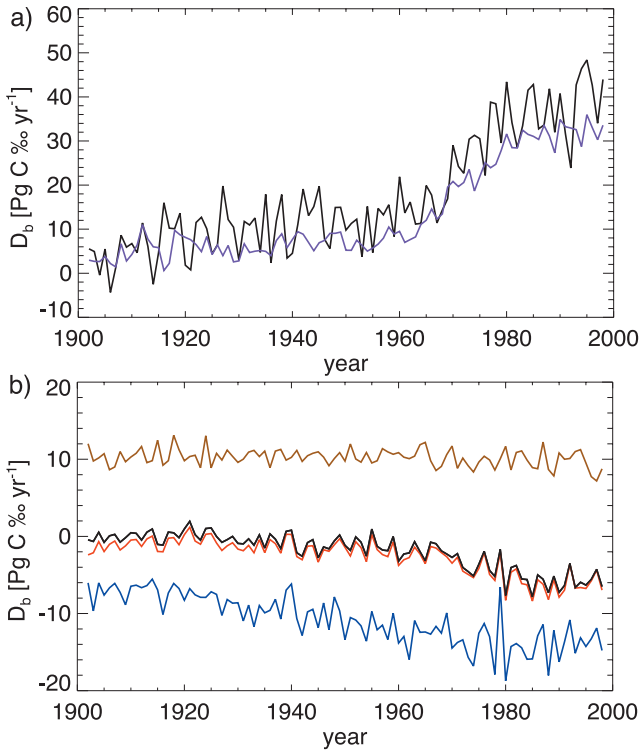


**Figure 12.** Global time series of (a) the modeled isotopic disequilibrium flux $D_b$ for the ISOVAR (black line) and ISOFIX (blue) simulations and of (b) the differences in global isotopic disequilibrium: ISOVAR without fire-ISOVAR (brown), ISOLU-ISOVAR (black), ISOLUC-ISOVAR (red) and ISOLUCP-ISOVAR (blue).

tively stable with a global value of around 8 Pg C yr$^{-1}$, whereas literature values of the biomass burning flux vary between 2 and 5 Pg C yr$^{-1}$ only [*Andreae*, 1991; *Malingreau and Zhuang*, 1998]. Therefore the impact of fire on the isotopic disequilibrium with a reduction of 10 Pg C‰ yr$^{-1}$ in $D_b$ seems to be overestimated. Including a land use scheme into the modeling framework leads to another reduction of 6 Pg C‰ yr$^{-1}$ because of the different treatment of the agricultural product pools (independent of climate) compared to the litter and soil pools. Including $C_4$ crops has only a marginal effect on the global disequilibrium flux, however, including also tropical $C_4$ pastures decreases $D_b$ by almost another 8 Pg C‰ yr$^{-1}$. *Townsend et al.* [2002] specified this 'reversed' isotopic disequilibrium flux due to the conversion from tropical $C_3$ forests to $C_4$ crops and pastures by using values of total conversion fluxes from *Houghton and Hacker*, [1995] and estimates of the isotopic signature of the heterotrophic respiration from model studies at point sites. Depending on the time since clearing (10 to 30 years) of the forests their average results for the 1990s lie between 8.8 and 15.8 Pg C yr$^{-1}$, respectively. *Ciais et al.* [2005] also quantified this land use change induced isotopic disequilibrium and obtained a value of 18.9 Pg C‰ yr$^{-1}$ using the same conversion fluxes from *Houghton and Hacker* [1995] but in a simple bookkeeping model [*Gitz and Ciais*, 2003]. Both *Townsend et al.* [2002] and *Ciais et al.* [2005] did not differentiate between $C_4$ crops and $C_4$ pastures. However, the marginal effect of $C_4$ crops in this study might be due to the fact that the area of croplands used by *Houghton and Hacker* [1995] is larger than by *Ramankutty and Foley* [1999] used for this study. Also, as LPJ is highly resolved both spatially and temporally, it is crucial to know the spatial and temporal distribution of tropical $C_4$ pastures as accurate as possible. Using a data set that is only decadally resolved, it could be that the total amount of converted area is underestimated and therefore the calculated additional decrease of 8 Pg C yr$^{-1}$ in the isotopic disequilibrium might be too low. On the other hand, aggregating the land use conversion fluxes on larger scales such as continental scales may lead to an overestimation of this flux and with it also the disequilibrium flux as reported by *Ciais et al.* [2005].

[33] As can be seen in Figure 12 and Figure 7, the ISOVAR simulation exhibits a much higher amount of interannual variability in the isotopic disequilibrium flux than the ISOFIX experiment. This large interannual variability is also apparent in the ISOVAR without fire and the land use experiments. The fluctuations are mainly due to the climate induced variability of the $^{13}$C discrimination during photosynthesis and by the variability in the relative share of $C_3$ versus $C_4$ photosynthesis (Figure 7). Year to year variations in the isotopic ratio of the respiration flux are strongly damped because of the relatively long residence time of carbon in the terrestrial pools. However, biomass burning has a potentially high influence on the interannual variability of the isotopic disequilibrium flux because it is believed that in certain years (with strong El Niño events) the burning flux is much higher than in other years [*Langenfelds et al.*, 2002; *Page et al.*, 2002] and may consume carbon of very distinct age (e.g., savannahs or forests). In fact, during the 1997/98 El Niño, satellite data of burned area show a systematic shift from tropical grassland fires to forest fires resulting in a depleted $^{13}$C net terrestrial flux [*Randerson et al.*, 2005]. As this additionally released carbon is mainly due to anthropogenic fire events it is not simulated by LPJ's fire module which only models natural fire events. The simulated interannual variability in the

**Table 3.** Comparison of Terrestrial $^{13}$C Quantities

| Period | Value | Source |
|---|---|---|
| | *Isotopic Disequilibrium $D_b$* | |
| 1988 | 0.43‰ | *Joos and Bruno* [1998] |
| | 0.33‰ | *Fung et al.* [1997] |
| | 0.49‰ | *Morimoto et al.* [2000] |
| | 0.59‰ | this study, ISOVAR |
| | 0.42‰ | this study, ISOLUCP |
| | *Isotopic Disequilibrium Flux $D_b$* | |
| 1970–1990 | 23.4 Pg % C yr$^{-1}$ | *Heimann and Meier-Reimer* [1996] |
| | 22.5 Pg % C yr$^{-1}$ | *Joos and Bruno* [1998] |
| | 33.4 Pg % C yr$^{-1}$ | this study, ISOVAR |
| | 19.2 Pg % C yr$^{-1}$ | this study, ISOLUCP |
| 1987 | 25.8 Pg % C yr$^{-1}$ | *Francey et al.* [1995] |
| | 33.6 Pg % C yr$^{-1}$ | this study, ISOVAR |
| | 22.2 Pg % C yr$^{-1}$ | this study, ISOLUCP |
| 1988 | 27.2 Pg % C yr$^{-1}$ | *Morimoto et al.* [2000] |
| | 41.8 Pg % C yr$^{-1}$ | this study, ISOVAR |
| | 23.8 Pg % C yr$^{-1}$ | this study, ISOLUCP |

natural carbon fire flux is rather low (less than 10% of the burning flux).

[34] A secular increase in $D_b$ after 1960 due to the increased burning of fossil fuel which depletes atmospheric $CO_2$ in $^{13}C$ is clearly visible. Figure 12a also shows that there is a difference of about 10 Pg C‰ $yr^{-1}$ in the isotopic disequilibrium flux between the ISOVAR and ISOFIX experiments at the end of the 1990s. This difference ($\approx$1/4 of the fossil fuel induced disequilibrium) results from the long-term trend in leaf discrimination in the ISOVAR experiment (see section 3.2.2), which is about 1/4 of the isotopic change in the atmosphere from fossil fuel use.

[35] As can be seen from the differences between the ISOVAR and the other experiments in the isotopic disequilibrium flux (Figure 12b), the positive trend is attenuated in the land use experiments. The specification of tropical $C_4$ pastures (ISOLUCP) has the strongest effect on this trend due to the larger area of low discriminating $C_4$ plants. In addition, there is a peak value in the difference between the ISOVAR and ISOLUCP experiments around 1980, after that year the difference is decreasing again. This is in agreement with the findings in the net carbon exchange in section 3.1 and results also from the decrease in the global area covered with tropical C4 pastures.

[36] *Heimann and Meier-Reimer* [1996] concluded from a sensitivity study that the value of the isotopic disequilibrium is one of the most crucial quantities in double deconvolution studies. The standard deviation of the global isotopic disequilibrium flux induced only by climate variability (i.e., the difference of $D_b$ between experiments with a variable discrimination during photosynthesis and the ISOFIX experiment) is larger than 5 Pg C‰ $yr^{-1}$ for all experiments. This value is in good agreement with the standard deviation in $D_b$ of 5.8 Pg C‰ $yr^{-1}$ reported by *Ito* [2003]. Because variations in the isotopic disequilibrium are mainly due to the variability in the leaf discrimination (as stated above) the spatial pattern of the variance in isotopic disequilibrium strongly resembles the patterns of the variance in $\Delta_{leaf}$ (see Figure 7).

## 4. Conclusions

[37] This study presents a process-based modeling framework for simulating terrestrial carbon and carbon 13 cycling. The influence of various quantities (climate, fire, land use and $C_4$ land use change) on the temporal and spatial patterns of the isotopic composition of the terrestrial biosphere has been analyzed. Variability in the atmosphere-biosphere $^{13}C$ exchange (both leaf discrimination and isotopic disequilibrium) on an interannual timescale is mainly influenced by climate variability and vegetation composition (fluctuations between $C_3$ and $C_4$ plants), whereas processes such as fire, land use and $C_4$ land use effect primarily the spatial distribution and the long-term trends. Taking the differences in the results between the ISOVAR and ISOLUCP experiments into account in double deconvolution studies we estimate that this could imply a shift of up to 1 Pg C $yr^{-1}$ from the inferred terrestrial sources to the ocean fluxes. This magnitude (1 Pg C $yr^{-1}$) of change in the carbon sink distribution between ocean and land represents approximately twice the size of the current uncertainties in the global carbon budget: a sink of 2.2 ± 0.5 Pg C $yr^{-1}$ and 0.9 ± 0.6 PG C $yr^{-1}$ [*Denman et al.*, 2007]. The history of conversion from natural vegetation to cultivation is an important boundary condition for estimating the effect of land conversion on the terrestrial isotopic composition but unfortunately not very well-known. This paper presents a sensitivity analysis of terrestrial $^{13}C$ cycling with respect to land use and $C_4$ land use using the data sets by *Ramankutty and Foley* [1999] and *Klein Goldewijk* [2001]. Using a different land use data set would yield different results especially for the disequilibrium fluxes as they seem to be most sensitive to the underlying land use pattern. For instance, the data set by *Houghton and Hacker* [1995] gives a larger area of croplands, which would translate into a smaller disequilibrium flux than estimated in this study if the amount of $C_4$ crops would scale accordingly. Therefore more information on the temporal and spatial distribution of land use, especially of $C_4$ crops and $C_4$ pastures distribution would help to quantify the impact of land use on atmospheric $\delta^{13}C$ and thus, strengthen the results of observationally analyses of the global carbon budget.

[38] **Acknowledgments.** We thank K. Klein Goldewijk for providing the historical pasture data sets and S. Sitch for providing the CCMLP land use LPJ version. This work was partly supported by the QUEST program of the Natural Environment Research Council, U.K.

## References

Andreae, M. O. (1991), Biomass burning: its history, use, and distribution and its impact on environmental quality and global change, in *Global biomass burning: atmospheric, climatic, and biospheric implications*, edited by J. S. Levine, pp. 3–21, MIT Press, Cambridge, USA.

Arneth, A., J. Lloyd, H. Santrukova, M. Bird, S. Grigoryev, B. Y. N. Kalaschnikov, G. Gleixner, and E.-D. Schulze (2002), Response of central Siberian Scots pine to soil water deficit and long-term trends in atmospheric $CO_2$ concentration, *Global Biogeochem. Cycles*, *16*(1), 1005, doi:10.1029/2000GB001374.

Bakwin, P. S., P. P. Tans, J. W. C. White, and R. J. Andres (1998), Determination of the isotopic ($^{13}C/^{12}C$) discrimination by terrestrial biology from a global network of observations, *Global Biogeochem. Cycles*, *12*, 555–562.

Battle, M., M. L. Bender, P. P. Tans, J. W. C. White, J. T. Ellis, T. Conway, and R. J. Francey (2000), Global carbon sinks and their variability inferred from atmospheric $O_2$ and $\delta^{13}C$, *Science*, *287*, 2467–2470.

Bert, D., S. W. Leavitt, and J. L. Dupouey (1997), Variations of wood Delta-C-13 and water-use efficiency of Abies Alba during the last century, *Ecology*, *78*, 1588–1596.

Bowling, D. R., D. D. Baldocchi, and R. K. Monson (1999), Dynamics of isotopic exchange of carbon dioxide in a Tennessee deciduous forest, *Global Biogeochem. Cycles*, *13*, 903–922.

Buchmann, N., and J. O. Kaplan (2001), Carbon isotope discrimination of terrestrial ecosystems - How well do observed and modeled results match?, in *Global biogeochemical cycles in the climate system*, edited by E.-D. Schulze, M. Heimann, S. Harrison, E. Holland, J. Lloyd, and I. C. Prentice, pp. 253–266, Academic Press, San Diego.

Buchmann, N., R. J. Brooks, L. B. Flanagan, and J. R. Ehleringer (1998), Carbon isotope discriminiation of terrestiral ecosystems, in *Stable Isotopes*, edited by H. Griffiths, pp. 203–222, BIOS Sci., Oxford.

Ciais, P., P. P. Tans, M. Trolier, J. W. C. White, and R. J. Francey (1995), A large northern hemisphere terrestrial $CO_2$ sink indicated by the $\delta^{13}C/^{12}C$ ratio of atmospheric $CO_2$, *Science*, *269*.

Ciais, P., et al. (1997), A three-dimensional synthesis study of 18O in atmospheric CO2. 1. Surface fluxes, *J. Geophys. Res.*, *102*, 5857–5872.

Ciais, P., P. Friedlingstein, D. S. Schimel, and P. P. Tans (1999), A global calculation of the $\delta^{13}C$ of soil respired carbon: Implications for the biospheric uptake of anthropogenic $CO_2$, *Global Biogeochem. Cycles*, *13*, 519–530.

Ciais, P., M. Cuntz, M. Scholze, F. Mouillot, P. Peylin, and V. Gitz (2005), Remarks on the use of $^{13}C$ and $^{18}O$ isotopes in atmospheric $CO_2$ to quantify

biospheric carbon fluxes, in *Stable Isotopes and Biosphere-Atmosphere Interactions*, edited by L. B. Flanagan, J. R. Ehleringer, and D. Pataki, pp. 235–267, Elsevier Academic Press, Amsterdam.

Craig, H. (1954), Carbon-13 in plants and the relationship between carbon-13 and carbon-14 variations in nature, *J. Geol.*, *62*, 115–149.

Denman, K. L., et al. (2007), Couplings between changes in the climate system and biogeochemistry, in *Climate Change 2007. The Physical Science Basis. Contribution of Working Group I to the Fourth Assessment Report of the Intergovernmental Panel on Climate Change*, edited by S. Solomon, D. Qin, M. Manning, Z. Chen, M. Marquis, K. B. Averyt, M. Tignor, H. L. Miller, Cambridge University Press, Cambridge, United Kingdom.

Duquesnay, A., N. Breda, M. Stievenard, and J. L. Dupouey (1998), Changes of tree-ring $\delta^{13}C$ and water-use efficiency of beech (Fagus sylvatica L.) in north-eastern France during the past century, *Plant Cell Environ.*, *21*, 565–572.

Ekblad, A., and P. Högberg (2001), Natural abundance of $^{13}C$ in $CO_2$ respired from forest soils reveals speed of link between tree photosynthesis and root respiration, *Oecologia*, *127*, 305–308.

Esser, G. (1995), Contribution of monsoon Asia to the carbon budget of the biosphere, past and future, *Vegetatio*, *121*, 175–188.

FAO (2002), FAOSTAT, internet version (http://apps.fao.org/), Food and Agricultural Organization of the United Nations, Rome.

Foley, J. (1995), An equilibrium model of the terrestrial carbon budget, *Tellus*, *47B*, 310–319.

Francey, R. J., P. P. Tans, C. E. Allison, I. G. Enting, J. W. C. White, and M. Trolier (1995), Changes in oceanic and terrestrial carbon uptake since 1982, *Nature*, *373*, 326–330.

Francey, R. J., C. E. Allison, D. M. Etheridge, C. M. Trudinger, I. G. Enting, M. Leuenberger, R. L. Langenfelds, E. Michel, and L. P. Steele (1999), A 1000-year high precision record of $\delta^{13}C$ in atmospheric $CO_2$, *Tellus*, *51B*, 170–193.

Fung, I., et al. (1997), Carbon 13 exchanges between the atmosphere and biosphere, *Global Biogeochem. Cycles*, *11*, 507–533.

Gitz, V., and P. Ciais (2003), Amplifying effects of land-use change on future atmospheric $CO_2$ levels, *Global Biogeochem. Cycles*, *17*(1), 1024, doi:10.1029/2002GB001963.

Heimann, M., and E. Meier-Reimer (1996), On the relations between the oceanic uptake of $CO_2$ and its carbon isotopes, *Global Biogeochem. Cycles*, *10*, 89–110.

Hemming, D. L., V. R. Switsur, J. S. Waterhouse, and T. H. E. Heaton (1998), Climate variation and the stable carbon isotope composition of tree ring cellulose: An intercomparison of Quercus robur, Fagus sylvatica and Pinus silvestris, *Tellus, Ser. B*, *50*, 25–33.

Houghton, R. A. (2003), Revised estimates of the annual net flux of carbon to the atmosphere from changes in land use and land management 1850–2000, *Tellus*, *55*, 378–390.

Houghton, R. A., and J. L. Hacker (1995), ORNL/CDIAC data set NDP-050.

Ito, A. (2003), A global-scale simulation of the CO2 exchange between the atmosphere and the terrestrial biosphere with a mechanistic model including stable carbon isotopes, 1953–1999, *Tellus*, *55*, 596–612.

Joos, F., and M. Bruno (1998), Long-trem variability of the terrestrial and oceanic carbon sinks and the budgets of the carbon isotopes $^{13}C$ and $^{14}C$, *Global Biogeochem. Cycles*, *12*, 277–295.

Kaplan, J. O., I. C. Prentice, and N. Buchmann (2002), The stable carbon isotope composition of the terrestrial biosphere, *Global Biogeochem. Cycles*, *16*(4), 1060, doi:10.1029/2001GB001403.

Keeling, C. D., R. B. Bacastow, A. F. Carter, S. C. Piper, T. P. Whorf, M. Heimann, W. G. Mook, and H. Roeloffzen (1989), A three-dimensional model of the atmospheric $CO_2$ transport based on observed winds: 1. Analysis of observational data, in *Aspects of Climate Variability in the Pacific and the Western Americas*, edited by D. H. Peterson, vol. 55, pp. 165–236, AGU, Washington, D. C.

Klein Goldewijk, K. (2001), Estimating global land use change over the past 300 years: The HYDE database, *Global Biogeochem. Cycles*, *15*, 417–434.

Klein Goldewijk, C. G. M., and J. J. Battjes (1997), A hundred year (1890–1990) database for integrated environmental assessments (HYDE, version 1.1), Tech. Rep. 422514002, National Institute of Public Health and the Environment (RIVM), Bilthoven, The Netherlands.

Langenfelds, R. L., R. J. Francey, B. C. Pak, L. P. Steele, J. Lloyd, C. M. Trudinger, and C. E. Allison (2002), Interannual growth rate variations of atmospheric $CO_2$ and its $\delta^{13}C$, $H_2$, $CH_4$ and CO between 1992 and 1999 linked to biomass burning, *Global Biogeochem. Cycles*, *16*(3), 1048, doi:10.1029/2001GB001466.

Leavitt, S. W., and A. Lara (1994), South American tree rings show declining $\delta^{13}C$ trend, *Tellus, Ser. B*, *46*, 152–157.

Lloyd, J., and G. Farquhar (1994), $^{13}C$ discrimination during $CO_2$ assimilation by the terrestrial biosphere, *Oecologia*, *99*, 201–215.

Lloyd, J., and J. A. Taylor (1994), On the temperature-dependence of soil respiration, *Funct. Ecol.*, *8*, 315–323.

Malingreau, J.-P., and Y. H. Zhuang (1998), Biomass burning: an ecosystem process of global significance, in *Asian change in the context of global climate change*, edited by J. Galloway and J. Mellilo, pp. 101–127, Cambridge University Press, Cambridge, U. K.

Marshall, J. D., and R. A. Monserud (1996), Homeostatic gas-exchange parameters inferred from $^{13}C/^{12}C$ in tree rings of conifers, *Oecologia*, *105*, 13–21.

McGuire, A. D., et al. (2001), Carbon balance of the terrestrial biosphere in the twentieth century: Analyses of $CO_2$, climate and land use effects with four process-based ecosystem models, *Global Biogeochem. Cycles*, *15*, 183–206.

Morimoto, S., T. Nakazawa, K. Higuchi, and S. Aoki (2000), Latitudinal distribution of atmospheric CO2 sources and sinks inferred by $\delta^{13}C$ measurements from 1985 to 1991, *J. Geophys. Res.*, *105*, 24,315–24,326.

New, M., M. Hulme, and P. Jones (2000), Representing twentieth-century space-time climate variability. Part II: Development of 1901–96 monthly grids of terrestrial surface climate, *J. Clim.*, *13*, 2217–2238.

Page, S., F. Siegert, J. O. Rieley, H.-D. V. Boehm, A. Jaya, and S. Limin (2002), The amount of carbon released from peat and forest fires in Indonesia during 1997, *Nature*, *420*, 61–65.

Prentice, I. C., et al. (2001), The carbon cycle and atmospheric carbon dioxide, in Climate Change 2001: The Scientific basis, edited by J. T. Houghton, Y. Ding, D. J. Griggs, M. Noguer, P. J. van der Linden, X. Dai, K. Maskell, and C. A. Johnson, pp. 183–237, Cambridge University Press, Cambridge, U. K.

Raffalli-Delerce, G., V. Masson-Delmotte, J. L. Dupouey, M. Stievenard, N. Breda, and J. M. Moisselin (2004), Reconstruction of summer droughts using tree-ring cellulose isotopes: A calibration study with living oaks from Brittany (western France), *Tellus, Ser. B*, *56*, 160–174.

Ramankutty, N., and J. Foley (1999), Estimating historical changes in global land cover: Croplands from 1700 to 1992, *Global Biogeochem. Cycles*, *13*, 997–1027.

Randerson, J., et al. (2005), Fire emissions from c3 and c4 vegetation and their influence on interannual variability of atmospheric co$_2$ and $\delta^{13}co_2$, *Global Biogeochem. Cycles*, *19*, GB2019, doi:10.1029/2004GB002366.

Rayner, P., I. Enting, R. Francey, and R. Langenfelds (1999), Reconstructing the recent carbon cycle from atmospheric $CO_2$, $\delta^{13}C$ and $O_2/N_2$ observations, *Tellus*, *B51*, 213–232.

Scholze, M., J. O. Kaplan, W. Knorr, and M. Heimann (2003), Climate and interannual variability of the atmosphere-biosphere $^{13}CO_2$ flux, *Geophys. Res. Lett.*, *30*(2), 1097, doi:10.1029/2002GL015631.

Sitch, S., et al. (2003), Evaluation of ecosystem dynamics, plant geography and terrestrial carbon cycling in the LPJ dynamic global vegetation model, *Global Change Biol.*, *9*, 161–185.

Still, C. J., J. A. Berry, G. J. Collatz, and R. S. DeFries (2003), Global distribution of $C_3$ and $C_4$ vegetation: Carbon cycle implications, *Global Biogeochem. Cycles*, *17*(1), 1006, doi:10.1029/2001GB001807.

Suits, N. S., A. S. Denning, J. A. Berry, C. J. Still, J. Kaduk, J. B. Miller, and I. T. Baker (2005), Simulation of carbon isotope discrimination of the terrestrial biosphere, *Global Biogeochem. Cycles*, *19*, GB1017, doi:10.1029/2003GB002141.

Thonicke, K., S. Venevsky, S. Sitch, and W. Cramer (2001), The role of fire disturbance for global vegetation dynamics: Coupling fire into a dynamic global vegetation model, *Glob. Ecol. Biogeogr.*, *10*, 661–677.

Townsend, A., G. Asner, J. White, and P. Tans (2002), Land use effects on atmospheric $^{13}C$ imply a sizable terrestrial $CO_2$ sink in tropical latitudes, *Geophys. Res. Lett.*, *29*(10), 1426, doi:10.1029/2001GL013454.

Wittenberg, U., and G. Esser (1997), Evaluation of the isotopic disequilibrium in the terrestrial biosphere by a global carbon isotope model, *Tellus*, *49B*, 263–269.

P. Ciais, Laboratoire des Sciences du Climat et de l'Environment, Bat 709, CE L'Orme des Merisiers, Gif sur Yvette, Cedex, France.

M. Heimann, Max-Planck-Institut für Biogeochemie, Hans-Knll-Strae 10, 07745 Jena, Germany.

M. Scholze, QUEST-Department of Earth Sciences, University of Bristol, Wills Memorial Building, Bristol BS8 1RJ, UK. (marko.scholze@bristol.ac.uk)